

Electron-optical phonon scattering in the quantum well of a HgTe/CdHgTe heterostructureV. Ya. Aleshkin^{1,2,*}, O. L. Domnina^{3,†} and M. S. Zholudev^{1,2,‡}¹*Department of Semiconductor Physics, Institute for Physics of Microstructures RAS, Nizhny Novgorod 603950, Russia*²*Lobachevsky State University of Nizhny Novgorod, Nizhny Novgorod 603950, Russia*³*Volga State University of Water Transport, Nizhny Novgorod 603950, Russia*

(Received 7 December 2023; revised 19 January 2024; accepted 2 February 2024; published 27 February 2024)

The optical phonon spectra in an HgTe quantum well surrounded by CdHgTe barriers are calculated, taking into account the contribution of free electrons to the dielectric permittivity of the quantum well. It is shown that free electrons not only change the phonon spectrum, but they can also change the number of branches of the surface optical phonons. The frequencies of the electron-optical phonon collisions, the wave-vector relaxation rates, and the energy relaxation rates are calculated for different temperatures and electron concentrations. The dependencies of the momentum and energy scattering frequencies on the electron kinetic energy are found.

DOI: [10.1103/PhysRevB.109.075307](https://doi.org/10.1103/PhysRevB.109.075307)**I. INTRODUCTION**

Scattering by optical phonons is one of the main mechanisms of relaxation of the energy and momentum of electrons whose energy exceeds the optical phonon energy. Such electrons can appear in the conduction band as a result of interband absorption of light with a photon energy significantly exceeding the band gap, or as a result of the impact of a strong electric field, or simply at the tail of the distribution function in the case when the temperature is of the same order as the optical phonon energy.

It is well known that in bulk semiconductors the presence of free electrons leads to a decrease in the frequency of the longitudinal optical phonon [1]. However, the dependence of the energy on the phonon wave vector does not change. In addition, the presence of free electrons changes the amplitude of the interaction of electrons with phonons due to screening of the phonon potential [2]. A completely different situation occurs in quantum wells. Free electrons in quantum wells not only change the frequencies of the optical phonons, but also change the dependence of the phonon energy on its wave vector [3]. Therefore, in this case one should expect a significantly greater influence of the presence of free carriers on the processes of electron scattering by the optical phonons.

In layers of polar semiconductors, including quantum wells, the characteristics of the optical phonons differ markedly from the characteristics of the optical phonons in bulk materials. If in cubic bulk semiconductors there are longitudinal and transverse optical phonons, then in semiconductor layers and quantum wells there are two other types of optical lattice vibrations: bulklike phonons and surface phonons [4–10]. This circumstance, as well as the two-dimensionality of electron motion in a quantum well, leads

to a noticeable difference in the characteristics of electron scattering by the optical phonons in bulk semiconductors and in quantum wells [11–22].

When studying the scattering of electrons by the optical phonons in quantum wells, the influence of the electron gas motion on the phonon spectrum is usually neglected [11–22]. The physical reason for the influence of the presence of electrons on lattice vibrations is that both lattice vibrations and electron density oscillations (plasma oscillations) create macroscopic electric fields that affect lattice vibrations and oscillations of the density of the electron gas. In Ref. [3] it was shown that the contribution to the dielectric of a quantum well due to free electron motion and interband electron transitions in HgTe quantum wells significantly changes the optical phonon spectrum. This should lead to a dependence of the probability of the electron-optical phonon scattering on the concentration of free electrons in the quantum well. To date, this dependence has not been studied.

Note that recently a number of works proposed a method for taking into account the influence of electrons in a quantum well on the phonon spectrum and on the electron-phonon interaction [23–25]. The approach proposed by the authors of these works consists of taking into account the influence of *static* screening by an electron gas of the electric field created by lattice vibrations. With this approach, as noted in [23], the dynamic effects of electron motion are not taken into account (i.e., the frequency dependence of the electron gas polarization was neglected). These effects lead to the existence of two-dimensional plasma oscillations. In this article it will be shown that plasmonic effects, which were neglected in these works, play a decisive role both in changing the spectrum of optical phonons and in changing the rate of electron-phonon scattering (including its increase for electrons with certain energies) at high electron concentrations in quantum wells.

Note that in [26] the influence of plasmonic effects on electron-optical phonon scattering in bulk semiconductors and in MoS₂ monolayers was studied. However, in [26] and in

*aleshkin@ipmras.ru

†o-domnina@yandex.ru

‡zholudev@ipmras.ru

[23–25], quantum wells consisting of one or several atomic monolayers were considered. In such quantum wells, the potential created by the electron-scattering phonon can be assumed to be constant inside the quantum well, since the width of the quantum well is much smaller than the scale of change in the electric potential. In the quantum wells considered in this work, the scale of change in the phonon potential is on the order of the quantum well width, and the change in the phonon potential inside the quantum well cannot be neglected. In addition, due to the small band gap of the quantum wells under consideration, a noticeable portion of the dielectric constant of the quantum well in the frequency range of the optical phonons is contributed by electronic transitions between two valence subbands and the lower subband of the conduction band [3]. In wide-gap quantum wells considered in [23–26], this contribution is insignificant.

The purpose of this work is to study the influence of free-carrier motion on the electron-optical phonon scattering using the example of the quantum-well HgTe/CdHgTe heterostructure. The article is organized as follows. In the second section, the spectra of the optical phonons in a 5 nm quantum well of the HgTe/Cd_{0.7}Hg_{0.3}Te heterostructure are calculated at three temperatures (4.2, 77, and 300 K) and four electron concentrations (0, 10¹⁰, 10¹¹, and 10¹² cm⁻²). In the third section, the phonon field is quantized, and expressions are given for calculating the frequency of the electron-optical phonon scattering, as well as expressions for finding the relaxation rates of electron momentum and energy. The fourth section presents the results of calculations of the frequencies of the electron-optical phonon scattering in an HgTe quantum well and the rates of relaxation of the electron momentum and energy. This section presents the calculated dependences of the relaxation frequencies of the electron momentum and energy on the electron kinetic energy. In addition, this section contains a discussion of the validity of the approximations used in the calculations. In the conclusion, the main results of the work are formulated, and physical phenomena are discussed in which the dependence of the electron-optical phonon scattering rate on the electron concentration in the quantum well plays an important role. We also discuss methods for observing the dependence of the optical phonon energy and the probability of electron-phonon scattering on the electron concentration in quantum wells.

II. OPTICAL PHONON SPECTRA

Let us consider the optical phonons in a 5 nm HgTe quantum well surrounded by Cd_{0.7}Hg_{0.3}Te barriers. We will assume that the structure is grown on the (013) plane of a thick CdTe buffer grown on a GaAs substrate. The technology for the growth of such structures has now been well developed [27,28]. Note that stimulated emission of radiation in the range of 3–31 μm wavelength was observed under optical excitation conditions in similar structures [29,30].

To calculate the phonon spectrum, we will use the dielectric continuum model. This model is well developed for quantum wells with both isotropic [4,9] and anisotropic [21,22] dielectric permittivity. In this model, to find the phonon spectrum, the dielectric permittivity of the quantum well and barriers is required. The dielectric permittivity of

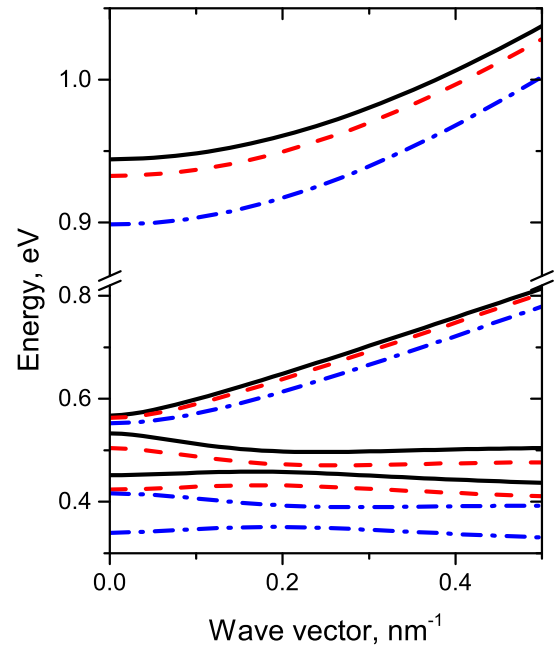


FIG. 1. Electron spectra in a 5 nm quantum well of the HgTe/Cd_{0.7}Hg_{0.3}Te heterostructure at three temperatures: 4.2 K (black solid lines), 77 K (red dotted line), and 300 K (blue dash-dotted line).

a quantum well is the sum of the electronic and lattice contributions. To calculate the contribution to the dielectric permittivity of a quantum well from the intraband and interband motion of electrons, it is necessary to find the electron states in the quantum well. To find these states, we used the Kane model, taking into account deformation effects. For simplicity, the calculations assumed that the quantum well was rectangular, i.e., the influence of the potential created by free carriers was not taken into account. Details of the calculation method can be found in [31].

Figure 1 shows the calculated electronic spectra in the quantum well of the structure under consideration for three temperatures: 4.2, 77, and 300 K. The figure shows that with increasing temperature the band gap increases, which is typical for such structures. In addition, it is clear from the figure that the distance between subbands in the conduction band is more than an order of magnitude greater than the optical phonon energies in HgTe (16 meV) and CdTe (21 meV). Note that the electron spectrum in the conduction band of the quantum well under consideration has a very weak anisotropy, which we will neglect.

When finding the dielectric permittivity tensor of a quantum well, we will use a number of simplifications. First, we neglect the spatial dispersion of the electron contribution to the dielectric permittivity. Secondly, when calculating the part of the dielectric permittivity due to the intrasubband electron motion, we will neglect electron collisions. Thirdly, we neglect the nonlocality of the dielectric permittivity of the quantum well [32]. To describe the dielectric permittivity tensor, we use the approximation proposed in [33] to describe the dielectric permittivity of bulk HgTe. In this approximation, only the diagonal components of the dielectric constant tensor

are nonzero. Their dependence on the cyclic frequency ω can be represented as the sum of four terms:

$$\kappa_{j,j}(\omega) = \kappa_{j,j}^{\infty} + \kappa_{j,j}^{\text{latt}}(\omega) + \kappa_{j,j}^{\text{inter}}(\omega) + \kappa_{j,j}^{\text{intra}}(\omega), \quad (1)$$

where the first term in Eq. (1) is due to electronic interband transitions between all zones, except for the size quantization subbands of the quantum well (transitions between far zones). The second term is associated with lattice vibrations. The third term is due to interband electron transitions between subbands of a quantum well (transitions between close subbands). The fourth term is due to the intrasubband electron motion. Note that only the third and fourth terms in Eq. (1) are anisotropic. By transitions between close subbands, we mean electronic transitions between subbands, the distance between which is of the order of the energy of the optical phonons in HgTe and CdTe. For the quantum well under consideration, these are transitions between the lower electron and two upper hole subbands. By transitions between far subbands, we mean transitions between subbands, the distance between which is much greater than the energy of the optical phonons in HgTe and CdTe. These are transitions to excited electronic subbands and transitions from hole subbands starting from the third one. The contribution of such transitions is implicitly taken into account in the first term of Eq. (1).

The part of the dielectric permittivity tensor caused by lattice vibrations and electronic transitions to far zones can be represented as [33]:

$$\kappa_{j,j}^{\infty} + \kappa_{j,j}^{\text{latt}}(\omega) = \delta_{j,j} \kappa_{\infty} \frac{\omega^2 - \omega_L^2}{\omega^2 - \omega_T^2}, \quad (2)$$

where κ_{∞} is the high-frequency permittivity of the quantum-well material (HgTe), and $\omega_{L,T}$ are the frequencies of the longitudinal and transverse optical phonons in bulk HgTe, respectively.

Within the framework of the approximations used, the expression for the third term of Eq. (1) can be written as:

$$\begin{aligned} \kappa_{j,j}^{\text{inter}}(\omega) = & -\frac{8\pi e^2 \hbar^2}{dS} \sum_{l,m,\mathbf{k}} \frac{|\mathbf{v}_{m,l}^j|^2}{\varepsilon_m(\mathbf{k}) - \varepsilon_l(\mathbf{k})} \\ & \times \frac{f_m(\mathbf{k}) - f_l(\mathbf{k})}{[\varepsilon_m(\mathbf{k}) - \varepsilon_l(\mathbf{k})]^2 - (\hbar\omega + i\alpha)^2}, \end{aligned} \quad (3)$$

where d is the quantum-well width, $\mathbf{v}_{m,l}^j$ is the j th component of the matrix element of the velocity operator between the initial electron state in the l th subband and the final electron state in the m th subband, e is the electron charge, \hbar is Planck's constant, \mathbf{k} is the electron wave vector, $f_l(\mathbf{k})$ is the distribution function of electrons in the l th subband, $\varepsilon_l(\mathbf{k})$ is the electron energy in the l subband, α is an infinitesimal positive value, and S is the quantum-well square. Expression (3) can be obtained by solving the Schrödinger equation for an electron moving in an electric field using the first order of perturbation theory.

The fourth term, taking into account the approximations made, has the form:

$$\kappa_{j,j}^{\text{intra}}(\omega) = \frac{4\pi e^2}{\hbar\omega^2 dS} \sum_{l,\mathbf{k}} \mathbf{v}_{l,l}^j \frac{\partial f_l(\mathbf{k})}{\partial k_j}, \quad (4)$$

where index l corresponds to subbands in the conduction band. Note that expression (4) is valid only for the isotropic electron dispersion. Expression (4) can be obtained by solving the collisionless Boltzmann equation for electrons moving in an oscillating electric field.

The barriers surrounding the quantum well are a bulk material with cubic symmetry, so its dielectric permittivity is isotropic. Since there are no free carriers there, and the CdHgTe barrier is a ternary alloy, then according to [19], the permittivity of the barrier can be written as:

$$\kappa_b(\omega) = \kappa_{\infty b} \frac{(\omega^2 - \omega_{\text{LHgTe}}^2)(\omega^2 - \omega_{\text{LCdTe}}^2)}{(\omega^2 - \omega_{\text{THgTe}}^2)(\omega^2 - \omega_{\text{TCdTe}}^2)}, \quad (5)$$

where $\kappa_{\infty b}$ is the high-frequency permittivity of $\text{Cd}_x\text{Hg}_{1-x}\text{Te}$, ω_{LHgTe} and ω_{THgTe} are the frequencies of the longitudinal and transverse HgTe-like optical phonons in $\text{Cd}_x\text{Hg}_{1-x}\text{Te}$, and ω_{LCdTe} and ω_{TCdTe} are the frequencies of the longitudinal and the transverse CdTe-like optical phonons in this material. The dependence of the longitudinal and transverse optical phonon frequencies on the composition of $\text{Cd}_x\text{Hg}_{1-x}\text{Te}$ is given in [34]. The dependence of $\kappa_{\infty b}$ on the composition of $\text{Cd}_x\text{Hg}_{1-x}\text{Te}$ is taken from [35].

Let the quantum well be located in the region $-d/2 < z < d/2$. The phase speed of the optical phonons, which can interact with electrons, is much less than the speed of light. Therefore, we can neglect retardation effects and describe the electric field created by lattice vibrations and electron density oscillations using the electric potential [9,21]. The potential created by the optical lattice vibrations propagating along the x axis with a wave vector q and frequency ω can be represented as:

$$\varphi_q(\mathbf{r}, t) = [c_q \exp(iqx - i\omega t) + \text{c.c.}] \Phi_q(z, \omega), \quad (6)$$

where the value c_q characterizes the amplitude of the potential, and c.c. denotes the complex conjugate term. The function $\Phi_q(z, \omega)$ can be found from the equation for electrical induction in a medium with an anisotropic dielectric permittivity depending on z [21]:

$$q^2 \kappa_{x,x}(z, \omega) \Phi(z, \omega) - \frac{\partial}{\partial z} \left(\kappa_{z,z}(z, \omega) \frac{\partial \Phi(z, \omega)}{\partial z} \right) = 0. \quad (7)$$

In the system under consideration, there is a plane of symmetry at $z = 0$, therefore the function $\Phi_q(z, \omega)$ can be either even in the argument z (even phonons) or odd (odd phonons). Only even phonons can participate in intrasubband electron scattering. Therefore, in what follows we restrict ourselves to considering only even phonons.

Similar to the case for a quantum well with an isotropic dielectric permittivity, the optical phonons in the system under consideration can be divided into bulklike and surface phonons. For bulklike even phonons, the function $\Phi_q(z, \omega)$ has the form [3]:

$$\Phi_q(z, \omega) = \begin{cases} \cos(\beta(\omega)qz), & |z| < d/2, \\ \cos\left(\frac{\beta(\omega)qd}{2}\right) \exp\left(\frac{qd}{2} - q|z|\right), & |z| > \frac{d}{2}, \end{cases} \quad (8)$$

where $\beta(\omega) = \sqrt{\frac{-\kappa_{x,x}(\omega)}{\kappa_{z,z}(\omega)}}$. Note that bulklike phonons exist in frequency intervals in which the condition $\kappa_{x,x}(\omega)\kappa_{z,z}(\omega) < 0$ is satisfied.

For surface even phonons, $\Phi_q(z, \omega)$ has the form [3]:

$$\Phi_q(z, \omega) = \begin{cases} \cosh(\gamma(\omega)qz), & |z| < d/2, \\ \cosh\left(\frac{\gamma(\omega)qd}{2}\right) \exp\left(\frac{d}{2} - q(|z|)\right), & |z| > \frac{d}{2}, \end{cases} \quad (9)$$

where $\gamma(\omega) = \sqrt{\frac{\kappa_{x,x}(\omega)}{\kappa_{z,z}(\omega)}}$. Surface phonons exist in frequency intervals in which the condition $\kappa_{x,x}(\omega)\kappa_{z,z}(\omega) > 0$ is satisfied. Note that similar expressions were obtained in [21,22] for GaN with a wurtzite structure, in which the phonon part of the dielectric permittivity is anisotropic.

The dependence of the wave vector on frequency for even bulklike phonons is found from the matching conditions of $\Phi(z, \omega)$ at the boundaries of the quantum well [3]:

$$q(\omega) = \frac{2}{d\beta(\omega)} \left[\arctan\left(\frac{\kappa_b(\omega)}{\kappa_{z,z}(\omega)\beta(\omega)}\right) + \pi n_1 \right], \quad (10)$$

where $n_1 = 0, 1, 2, \dots$. A similar dependence for even surface phonons can be represented as:

$$q(\omega) = \frac{2}{d\gamma(\omega)} \operatorname{atanh}\left(\frac{-\kappa_b(\omega)}{\gamma(\omega)\kappa_{z,z}(\omega)}\right). \quad (11)$$

Figure 2 shows the calculated optical phonon spectra in a quantum well at temperatures of 4.2, 77, and 300 K for four electron concentrations. Solid black lines correspond to bulklike phonons with $n_1 = 0$, and dashed black lines correspond to bulklike phonons with $n_1 = 1$. The spectra of bulklike phonons with $n_1 > 1$ are not given, since they make a small contribution to electron scattering. Red lines correspond to surface phonons. The figure shows how the spectrum of bulklike phonons changes greatly with increasing electron concentration. For electron concentrations of 0 and 10^{10} cm^{-2} , bulklike phonons have a weak dependence of energy on the wave vector, similar to the dependence of the optical phonon energy on the wave vector in a bulk material. For a quantum well with electron concentrations of 10^{11} and 10^{12} cm^{-2} , the dielectric permittivity of the quantum well is mainly determined by the contribution of free carriers. This circumstance dramatically changes the dependence of the phonon energy on the wave vector for bulklike phonons. In this case, it is more correct to call such excitations plasmon-phonons [36]. Similar excitations at the interface of a doped semiconductor and vacuum in [37] are called the plasma-phonon mode.

From Fig. 2 it can be seen that a change in the electron concentration affects the number of branches of surface phonons and their dispersion laws. So, for example, at an electron concentration of 10^{10} cm^{-2} there are three branches of the even surface optical phonons, and at the remaining concentrations considered there are two branches. The highest energy of the surface phonons at an electron concentration of 10^{10} cm^{-2} slightly exceeds 20 meV, and at concentrations of 10^{11} and 10^{12} cm^{-2} no more than 17 meV. In addition, the high-frequency surface plasmon for electron concentrations of 0 and 10^{10} cm^{-2} is a backward wave, and for electron

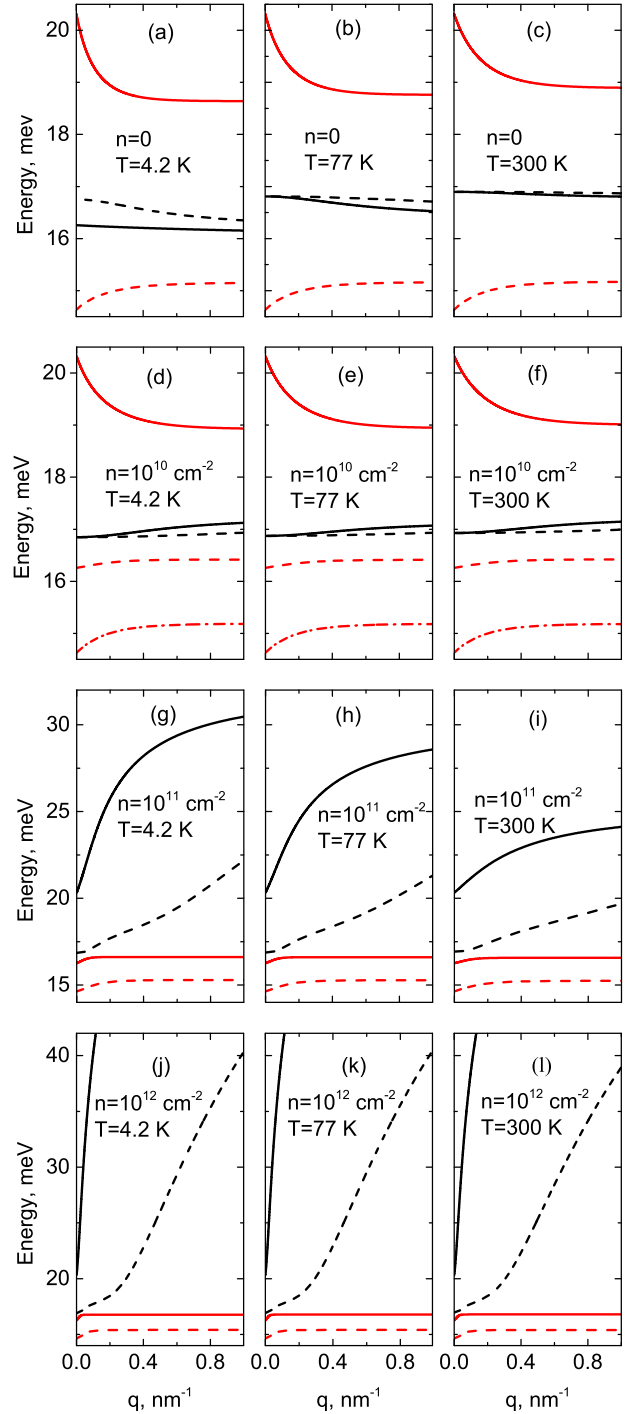


FIG. 2. Dependences of the energies of the even optical phonons on the wave vector for four electron concentrations at $T = 4.2, 77,$ and 300 K . Black solid lines correspond to the bulklike phonons with $n_1 = 0$, black dashed lines correspond to the bulklike phonons with $n_1 = 1$, and red lines correspond to the surface phonons. Panels (a)–(c) correspond to zero electron concentration, (d)–(f) to 10^{10} cm^{-2} , (g)–(i) to 10^{11} cm^{-2} , and (j)–(l) to 10^{12} cm^{-2} .

concentrations of 10^{11} and 10^{12} cm^{-2} it is wave with normal dispersion.

From Fig. 2 it can be seen that temperature changes have little effect on the phonon spectra. This influence is due to a

change in the contribution to the dielectric constant of the third and fourth terms in the formula (1) due to the temperature dependence of the band gap and electron effective mass in the conduction band of the quantum well. Note that in Eqs. (2) and (5) we neglected the temperature dependences of the optical phonon frequencies and κ_{∞} , $\kappa_{\infty b}$.

III. QUANTIZATION OF THE OPTICAL PHONON FIELD IN A QUANTUM WELL

Using the well-known expression for the energy of electromagnetic oscillations [38], the Hamiltonian of the optical phonon with wave vector q can be represented as:

$$H_q = \frac{S}{4\pi} \left[\frac{d\omega\kappa_b(\omega)}{d\omega} \int_{d/2}^{\infty} dz (\bar{E}_x^2 + \bar{E}_z^2) + \frac{d\omega\kappa_{xx}(\omega)}{d\omega} \int_0^{d/2} dz \bar{E}_x^2 + \frac{d\omega\kappa_{zz}(\omega)}{d\omega} \int_0^{d/2} dz \bar{E}_z^2 \right], \quad (12)$$

where $E_{x,z}$ are the components of the electric field created by the phonon, and the overbar denotes time averaging. In formula (12) we neglected the contribution of the magnetic field to the Hamiltonian. This approximation is valid in the quasistatic case, when the phase velocity of the phonon is much less than the speed of light. Phonons for which this approximation is wrong have a very small wave vector and do not take part in electron scattering.

Using the expressions for the potential (6), (8), and (9) and performing integration, formula (12) can be rewritten as:

$$H_q = c_q c_q^* F_q(\omega), \quad (13)$$

where the sign “*” denotes complex conjugation. The functions $F_q(\omega)$ for bulklike and surface phonons are given in the expressions (14) and (15), respectively,

$$F_q(\omega) = \frac{Sq}{8\pi} \left\{ 4 \frac{d\omega\kappa_b(\omega)}{d\omega} \cos^2(\beta(\omega)qd/2) + \frac{d\omega\kappa_{xx}(\omega)}{d\omega} \left[qd + \frac{\sin(\beta(\omega)qd)}{\beta(\omega)} \right] + \frac{d\omega\kappa_{zz}(\omega)}{d\omega} \beta(\omega) [\beta(\omega)qd - \sin(\beta(\omega)qd)] \right\}, \quad (14)$$

$$F_q(\omega) = \frac{Sq}{8\pi} \left\{ 4 \frac{d\omega\kappa_b(\omega)}{d\omega} \cosh^2(\gamma(\omega)qd/2) + \frac{d\omega\kappa_{xx}(\omega)}{d\omega} \left[qd + \frac{\sinh(\gamma(\omega)qd)}{\gamma(\omega)} \right] + \frac{d\omega\kappa_{zz}(\omega)}{d\omega} \gamma(\omega) [-\gamma(\omega)qd + \sinh(\gamma(\omega)qd)] \right\}. \quad (15)$$

By introducing the generalized coordinate Q_q and the generalized momentum P_q , we reduce the Hamiltonian (12) to the Hamiltonian of a harmonic oscillator:

$$H_q = (P_q^2 + \omega^2 Q_q^2)/2, \quad (16)$$

where:

$$Q_q = \frac{1}{\omega} \sqrt{\frac{F_q(\omega)}{2}} (c_q + c_q^*), \quad P_q = -i \sqrt{\frac{F_q(\omega)}{2}} (c_q - c_q^*). \quad (17)$$

Let us now introduce the operators of creation and annihilation of phonons a_q^+ , a_q :

$$a_q = \sqrt{\frac{\omega}{2\hbar}} (Q_q + iP_q/\omega), \quad a_q^+ = \sqrt{\frac{\omega}{2\hbar}} (Q_q - iP_q/\omega). \quad (18)$$

Using the creation and annihilation operators, we find the potential operator of the optical phonon with wave vector q :

$$\hat{\varphi}_q(\mathbf{r}, t) = \Phi_q(z) \sqrt{\frac{\hbar\omega}{F_q(\omega_q)}} (a_q \exp(i\mathbf{q}\mathbf{r} - i\omega_q t) + a_q^+ \exp(-i\mathbf{q}\mathbf{r} + i\omega_q t)), \quad (19)$$

where $\Phi_q(z) = \Phi_q(z, \omega_q)$, and ω_q is the frequency of the phonon with wave vector q .

We will assume that electrons interact with the optical phonons according to the Fröhlich mechanism [39], which is the only mechanism for the interaction of electrons with the optical phonons in the Γ -valley of the conduction band of cubic semiconductors [2]. In this case, electrons are scattered by the macroscopic electric potential created by the optical vibrations of the lattice. The probability of scattering of the electron with wave vector \mathbf{k} from the l th subband (subband index includes spin) into the m subband with the emission of a phonon with wave vector \mathbf{q} can be written as [2]:

$$W_{\mathbf{k},l \rightarrow \mathbf{k}-\mathbf{q},m}^+ = \frac{2\pi}{\hbar} e^2 |\varphi_{\mathbf{k}-\mathbf{q},m;\mathbf{k},l}|^2 (N_q + 1) (1 - f_m(\mathbf{k} - \mathbf{q})) \times \delta(\varepsilon_l(\mathbf{k}) - \varepsilon_m(\mathbf{k} - \mathbf{q}) - \hbar\omega_q), \quad (20)$$

where $\varphi_{\mathbf{k}-\mathbf{q},m;\mathbf{k},l}$ is the matrix element of the potential operator, and N_q is the number of phonons with wave vector \mathbf{q} . Furthermore, we will assume that the phonon distribution is equilibrium, $N_q = [\exp(\hbar\omega_q/k_B T) - 1]^{-1}$, where k_B is Boltzmann's constant.

A similar expression for the probability of electron scattering with phonon absorption can be written as:

$$W_{\mathbf{k},l \rightarrow \mathbf{k}+\mathbf{q},m}^- = \frac{2\pi}{\hbar} e^2 |\varphi_{\mathbf{k}+\mathbf{q},m;\mathbf{k},l}|^2 N_q (1 - f_m(\mathbf{k} + \mathbf{q})) \times \delta(\varepsilon_l(\mathbf{k}) - \varepsilon_m(\mathbf{k} + \mathbf{q}) + \hbar\omega_q). \quad (21)$$

The scattering frequency of an electron with a wave vector \mathbf{k} from the l th subband is equal to:

$$W_l(k) = \sum_{\mathbf{q},m} (W_{\mathbf{k},l \rightarrow \mathbf{k}-\mathbf{q},m}^+ + W_{\mathbf{k},l \rightarrow \mathbf{k}+\mathbf{q},m}^-). \quad (22)$$

Important relaxation characteristics of an electron are the relaxation rate of the wave vector (momentum) and energy. The relaxation rate of the wave vector can be represented in the following form [2]:

$$\mathbf{P}_l(k) = \sum_{\mathbf{q},m} \mathbf{q} (W_{\mathbf{k},l \rightarrow \mathbf{k}-\mathbf{q},m}^+ - W_{\mathbf{k},l \rightarrow \mathbf{k}+\mathbf{q},m}^-). \quad (23)$$

Due to the isotropy of the electronic and phonon spectra, the vector $\mathbf{P}_l(k)$ is directed along the vector \mathbf{k} . Note that for

positive values of $\mathbf{P}_l(k)$ the electron wave vector decreases as a result of collisions, and for negative values it increases.

The energy relaxation rate can be represented as [2]:

$$Q_l(k) = \sum_{\mathbf{q}, m} \hbar \omega_q (W_{\mathbf{k}, l \rightarrow \mathbf{k}-\mathbf{q}, m}^+ - W_{\mathbf{k}, l \rightarrow \mathbf{k}+\mathbf{q}, m}^-). \quad (24)$$

IV. RATES OF ELECTRON-OPTICAL PHONON SCATTERING

Figure 3 shows the dependence of the frequencies of the electron-optical phonon scattering on the electron kinetic energy. The blue dotted lines correspond to the total scattering frequencies. The designation of the remaining lines corresponds to the designation of the lines in Fig. 2. From the figure it is clear that the main contribution to the frequency of the electron-optical phonon scattering at electron concentrations of 0 and 10^{10} cm^{-2} comes from scattering on the high-frequency branch of the surface phonons (red solid line). For electron concentrations of 10^{11} and 10^{12} cm^{-2} the main contribution to the scattering under consideration comes from scattering from a bulklike mode with $n_1 = 0$ (solid black line). It can be seen that the contribution of the bulklike mode with $n_1 = 1$ (dashed black line) to scattering is much less than the contribution of the bulklike mode with $n_1 = 0$. Calculations show that bulklike modes with $n_1 > 1$ make an even smaller contribution to scattering due to the smallness of the corresponding overlap integral in $\varphi_{\mathbf{k}-\mathbf{q}, m; \mathbf{k}, l}$, so we do not consider them.

At a temperature of $T = 4.2 \text{ K}$, scattering by the optical phonons occurs only due to the spontaneous emission of phonons. From panels (a), (d), (g), and (j) it is clearly seen that with increasing electron concentration, the minimum energy of an electron that can emit the optical phonon increases. This is due to the Pauli exclusion principle, which prohibits scattering into the final occupied state. That is, for such scattering, the electron energy at $T = 4.2 \text{ K}$ must be no less than the sum of the Fermi energy and the phonon energy (if the phonon dispersion is weak). At $T = 4.2 \text{ K}$, the Fermi energies, measured from the bottom of the subband, are equal to 3, 22, and 108 meV for concentrations of 10^{10} , 10^{11} , and 10^{12} cm^{-2} , respectively.

At temperatures of 77 and 300 K, the presence of a step in the dependence of the scattering frequency on the electron energy is visible. Scattering to the left of the step is caused by the processes of phonon absorption, and to the right of it by the sum of the processes of absorption and emission of phonons. The scattering probability to the right of the step changes slightly as the temperature changes from 4.2 to 77 K, but increases noticeably as the temperature changes from 77 to 300 K at a fixed electron concentration. Note that the scattering under consideration occurs with spin conservation, i.e., during scattering, the index l is preserved.

Figure 4 shows the dependences of the wave-vector relaxation rate [panels (a), (c), (e)] and the momentum relaxation frequency ν_p [panels (b), (d), (f)] on the electron kinetic energy. The momentum relaxation frequency was determined from the relation:

$$P(k) = k\nu_p. \quad (25)$$

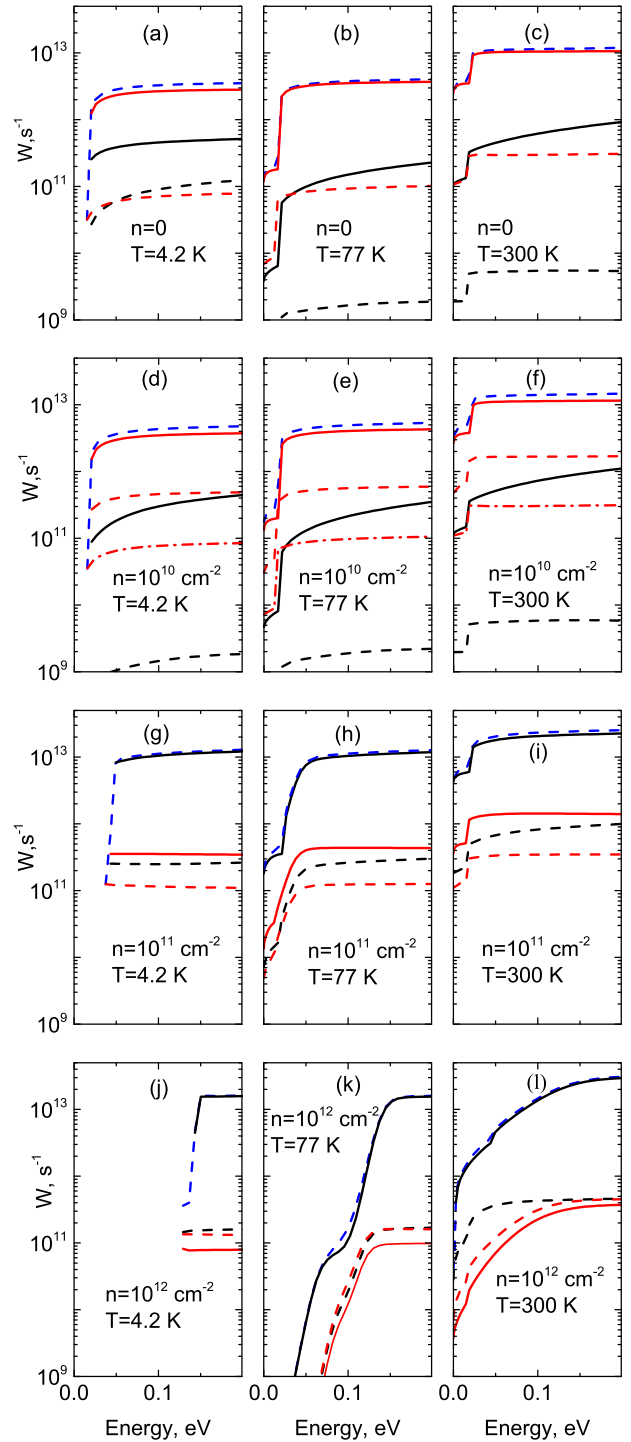


FIG. 3. Dependences of the frequency of the electron-optical phonon scattering for various electron concentrations and temperatures. The blue dashed lines correspond to the total frequency of scattering by all the optical phonons. For frequencies of scattering by certain types of phonons, the same notation is used as in Fig. 2. For example, the frequency for scattering by a bulklike mode with $n_1 = 0$ is indicated by a solid black line.

In Eq. (25), the subscript l is omitted, since scattering occurs with spin conservation. Note that at temperatures of 77 and 300 K in the electron energy region, where only phonon absorption is possible, the wave-vector relaxation

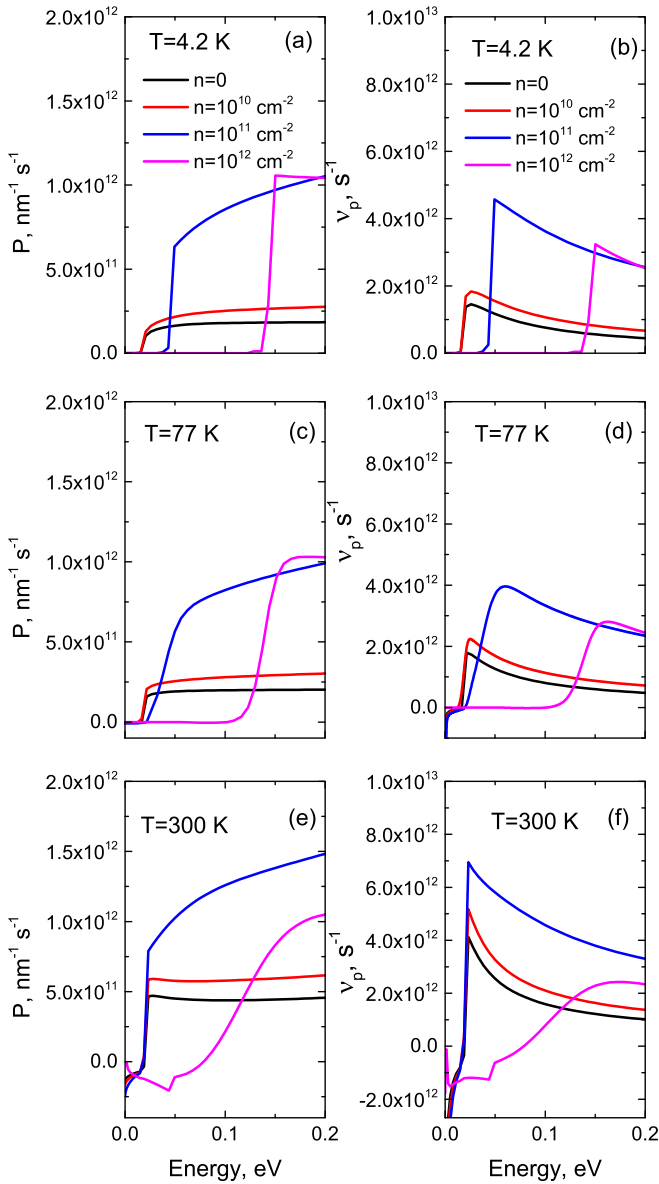


FIG. 4. Dependences of the wave-vector relaxation rates [panels (a), (b), (e)] and the momentum relaxation frequency (b), (d), (f) on the electron kinetic energy for various electron concentrations and temperatures. The correspondence between line colors and electron concentrations is shown in panels (a) and (b).

rates and the momentum relaxation frequency are negative. This happens because in absorption processes during polar scattering, processes with forward scattering prevail, i.e., with a minimal phonon wave vector, which is typical for polar scattering [2].

From Fig. 4 it is clear that an increase in the electron concentration from 10^{10} to 10^{11} cm^{-2} leads to a sharp increase in the relaxation rate of the wave vector and the momentum relaxation frequency. The reason for this is a change in the type of phonon, which makes the main contribution to scattering from the high-frequency surface to a bulklike one (see Fig. 3). Let us note an increase in the relaxation rate of the wave vector with increasing temperature. In addition, the momentum relaxation frequency for the electron-optical

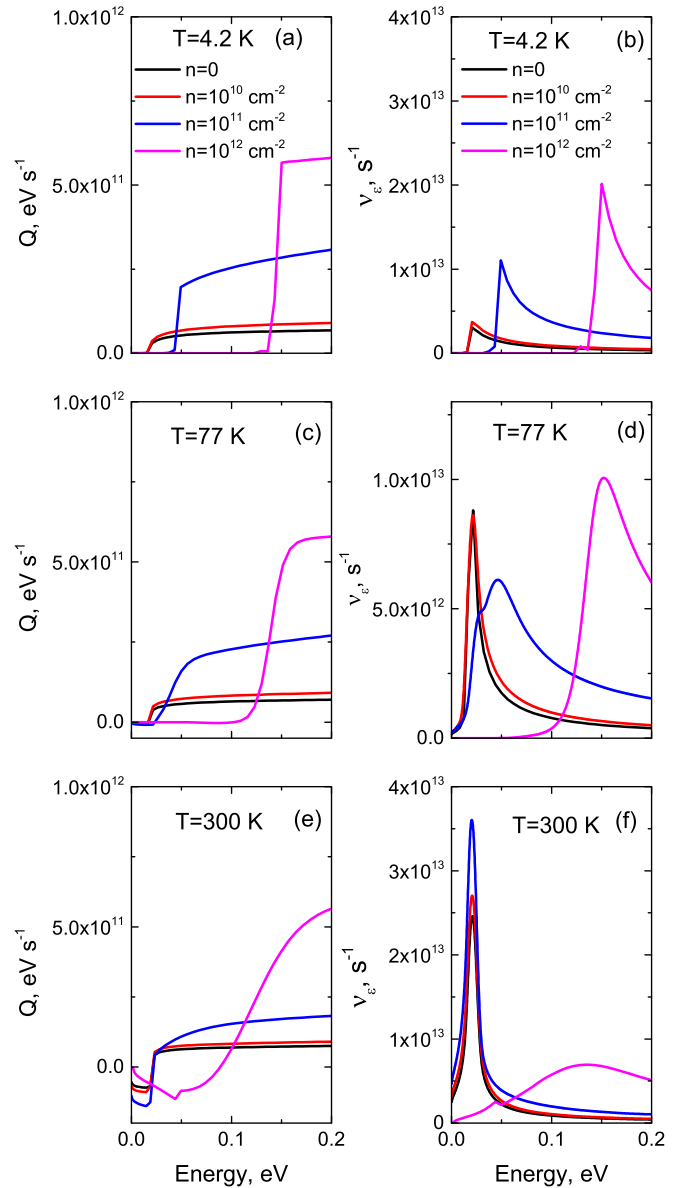


FIG. 5. Dependences of energy relaxation rates [panels (a), (c), (e)] and energy relaxation frequencies [panels (b), (d), (f)] on the electron kinetic energy for various electron concentrations and temperatures. The correspondence between line colors and electron concentrations is shown in panels (a) and (b).

phonon scattering has its maximum at energies corresponding to the onset of phonon emission processes.

Figure 5 shows the dependences of the electron kinetic energy relaxation rate [panels (a), (c), (e)] and the energy relaxation frequency ν_{ε} [panels (b), (d), (f)] for scattering by the optical phonons. The frequency of energy relaxation was found from the relation:

$$Q(k) = [\varepsilon(k) - \varepsilon^*] \nu_{\varepsilon}, \quad (26)$$

where ε^* is the energy at which $Q = 0$. Just like Eq. (25), the index l is omitted from the formula (26).

From Fig. 5 it is clear that with increasing electron concentration, the rate of energy relaxation increases in those regions where the emission of the optical phonons is

possible. The maximum frequency of energy relaxation is realized in the case when $\varepsilon = \varepsilon^*$. For $T = 4.2$ it was assumed that ε^* is the energy at which scattering was turned on. With increasing temperature, the rate of energy relaxation in the region where it is negative increases in absolute value, which is due to an increase in the phonon absorption frequency.

Let us now list the main approximations used in the work and discuss their applicability. In our calculations, we neglected the finite lifetime of the optical phonons due to the anharmonicity of lattice vibrations. Since the inverse lifetime of the optical phonons due to anharmonicity is much less than the frequency of the optical phonons, it has little effect on scattering processes. When calculating the electronic contribution to the dielectric constant of the quantum well, we neglected electron collisions and spatial dispersion of electronic polarizability. The frequency of electronic collisions is much lower than the frequency of the optical phonons, so we can assume that taking it into account will have little effect on the considered phonon spectra and the considered scattering processes. Taking into account the spatial dispersion of electronic polarizability will significantly change the phonon spectrum at large wave vectors, in the case when it is mainly determined by electronic polarizability (i.e., for electron concentrations of 10^{11} and 10^{12} cm $^{-2}$) [36]. However, due to the polar mechanism of the considered scattering, scattering processes with low momentum transfer are most likely. Therefore, taking into account the spatial dispersion of electronic polarizability will not change the qualitative results obtained, although it certainly requires a separate consideration that is beyond the scope of this work.

When considering scattering, we also neglected scattering by the optical phonons from barriers occupying the half-space. These phonons have frequencies that coincide with the frequencies of the longitudinal phonons in the barrier material, i.e., they are bulklike. The potential they create is zero in a quantum well. The wave functions of electrons in the lower size quantization subband in the conduction band of the quantum well weakly penetrate in the barrier. For this reason, the overlap integral of the potential created by such phonons and the electronic wave functions is rather small, which leads to a low probability of scattering.

V. CONCLUSION

In conclusion, we briefly list the main results obtained in this work, and we discuss the observed consequences of the dependence of electron-optical phonon scattering on the electron concentration in a quantum well, which was considered in this work. In addition, methods for experimental observation of phonon spectra and electron-optical phonon scattering times are discussed.

(1) The optical phonon spectra were found in the HgTe/Cd $_{0.7}$ Hg $_{0.3}$ Te heterostructure with a 5 nm quantum well at three temperatures (4.2, 77, and 300 K) and four electron concentrations (0, 10^{10} , 10^{11} , and 10^{12} cm $^{-2}$). It is shown that the presence of electrons in the conduction band of a quantum well significantly affects the dispersion of both surface and bulklike phonons. In addition, the presence of electrons affects the number of surface phonon modes: at

electron concentrations of 0, 10^{11} , and 10^{12} cm $^{-2}$ there are only two surface modes in the system under consideration, and at a concentration of 10^{10} cm $^{-2}$ there are three surface modes.

(2) The dependences of the electron-optical phonon scattering frequency on the electron kinetic energy are found. It is shown that for electron concentrations of 0 and 10^{10} cm $^{-2}$ the main mechanism of electron scattering by the optical phonons is scattering by a high-frequency surface mode. For concentrations of 10^{11} and 10^{12} cm $^{-2}$ the main scattering mechanism is scattering by a bulklike mode with $n_1 = 0$. It is shown that an increase in the number of the bulklike mode n_1 leads to a decrease in the probability of electron scattering from this mode.

(3) The dependences of the relaxation rates of the wave vector and energy on the electronic kinetic energy are calculated. The dependences of the momentum relaxation frequency and electron energy on its kinetic energy were found.

Let us now discuss the observable consequences resulting from the dependence of the electron-optical phonon scattering on the electron concentration in the quantum well. The first thing we can pay attention to is the dependence of electron mobility on the electron concentration at high temperatures, when the temperature is on the order of the energy of optical phonons. In this case, electron scattering by optical phonons significantly affects the electron mobility. In addition, one should expect a change in the dependence of mobility on temperature with changes in the electron concentration. However, it should be noted that there are several factors, in addition to the probability of scattering by the optical phonons, that influence the change in electron mobility with increasing electron concentration. These factors include the nonparabolic nature of the electron spectrum in an HgTe quantum well due to which the average effective mass of electrons increases with increasing electron concentration. In addition, due to improved screening, with increasing electron concentration, the probabilities of scattering by a charged impurity and acoustic phonons decrease. Therefore, the study of the dependence on the electron concentration under these conditions requires separate consideration. Note that in Ref. [26], the dependence of electron mobility on the electron concentration in MoS $_2$ monolayers was studied. However, that work did not take into account the scattering of electrons by acoustic phonons and charged impurities.

The second thing that should be noted is the dependence of the current on the electric field under conditions of electronic heating, in a situation in which Ohm's law stops working. In this case, the dependence of the current on the electric field is determined by the dependencies of the relaxation times of the momentum and energy on the average electron energy [40]. As was shown in this work, these times change with increasing electron concentration. This should lead to a change in the dependence of the current on the electric field when the electron concentration changes in strong fields, when Ohm's law does not work.

Third, an increase in the probability of electron-optical phonon scattering will lead to a decrease in the heating of the electron gas in a high electric field, and, consequently, to an

increase in the interband breakdown field with an increase in the electron concentration (although here the Pauli principle works in the same direction, effectively increasing the band gap). However, studying the influence of electron concentration both on the dependence of the current on the electric field in heating fields and on the interband breakdown field requires separate consideration and is beyond the scope of this work.

Let us now discuss how the phenomena considered can be observed. The dependence of the energy of the optical phonons in quantum wells at small wave vectors on the electron concentration can be observed using Raman scattering. A detailed discussion of issues related to such observations can be found in Ref. [1]. In addition, the dependence of the optical

phonon energy on the wave vector can be studied using the methods used to study surface waves [37].

The probabilities of electron scattering with different energies by the optical phonons can be studied using the pump-probe method [25] or by observing the Hanle effect in the study of hot photoluminescence [41].

Data underlying the results presented in this paper are not publicly available at this time but may be obtained from the authors upon reasonable request.

ACKNOWLEDGMENT

The work was supported by the Russian Science Foundation (Project No. 22-72-10111).

-
- [1] P. Y. Yu and M. Cardona, *Fundamentals of Semiconductors. Physics and Material Properties*, 4th ed. (Springer, New York, 2010).
- [2] V. F. Gantmacher and I. B. Levinson, *Carrier Scattering in Metals and Semiconductors* (North-Holland, New York, 1987).
- [3] V. Y. Aleshkin and M. S. Zholudev, *Physica E* **157**, 115863 (2024).
- [4] F. Fuchs and K. L. Kliewer, *Phys. Rev.* **140**, A2076 (1965).
- [5] E. P. Pokatilov and S. I. Beril, *Phys. Status Solidi B* **110**, 75 (1982).
- [6] F. Bechstedt and R. Enderlein, *Phys. Status Solidi B* **131**, 53 (1985).
- [7] L. Wendler and R. Pechstedt, *Phys. Status Solidi B* **141**, 129 (1987).
- [8] R. Enderlein, F. Bechstedt, and G. Gerecke, *Phys. Status Solidi B* **148**, 173 (1988).
- [9] K. Huang and B. Zhu, *Phys. Rev. B* **38**, 13377 (1988).
- [10] H. Yildirim, *Phys. Lett. A* **385**, 126977 (2021).
- [11] A. A. Lucas, E. Kartheuser, and R. G. Badro, *Phys. Rev. B* **2**, 2488 (1970).
- [12] E. P. Pokatilov and S. I. Beril, *Phys. Status Solidi B* **118**, 567 (1983).
- [13] J. K. Jain and S. Das Sarma, *Phys. Rev. Lett.* **62**, 2305 (1989).
- [14] N. Mori and T. Ando, *Phys. Rev. B* **40**, 6175 (1989).
- [15] H. Rucker, E. Molinari, and P. Lugli, *Phys. Rev. B* **44**, 3463 (1991).
- [16] H. Rucker, E. Molinari, and P. Lugli, *Phys. Rev. B* **45**, 6747 (1992).
- [17] X. T. Zhu, H. G. Goronkin, N. Maracas, R. Droopad, and M. A. Stroschio, *Appl. Phys. Lett.* **60**, 2141 (1992).
- [18] I. Lee, S. M. Goodnick, M. Gulia, E. Molinari, and P. Lugli, *Phys. Rev. B* **51**, 7046 (1995).
- [19] R. Zheng and M. Matsuura, *Phys. Rev. B* **60**, 4937 (1999).
- [20] J. Požela, A. Namajunas, K. Pozela, and V. Juciene, *Semiconductors* **33**, 956 (1999).
- [21] B. C. Lee, K. W. Kim, M. A. Stroschio, and M. Dutta, *Phys. Rev. B* **58**, 4860 (1998).
- [22] S. M. Komirenko, K. W. Kim, M. A. Stroschio, and M. Dutta, *Phys. Rev. B* **61**, 2034 (2000).
- [23] F. Macheda, T. Sohler, P. Barone, and F. Mauri, *Phys. Rev. B* **107**, 094308 (2023).
- [24] T. Sohler, M. Gibertini, and M. J. Verstraete, *Phys. Rev. Mater.* **5**, 024004 (2021).
- [25] Z. Chen, J. Sjakste, J. Dong, A. Taleb-Ibrahimi, J.-P. Rueff, A. Shukla, J. Peretti, E. Papalazarou, M. Marsi, and L. Perfetti, *Proc. Natl. Acad. Sci. USA* **117**, 21962 (2020).
- [26] A. Hauber and S. Fahy, *Phys. Rev. B* **95**, 045210 (2017).
- [27] N. N. Mikhailov, R. R. Smirnov, S. A. Dvoretzky, Y. G. Sidorov, V. A. Shvets, E. V. Spesivtsev, and S. V. Rykhliitski, *Int. J. Nanotechnol.* **3**, 120 (2006).
- [28] S. Dvoretzky, N. Mikhailov, Y. Sidorov, V. Shvets, S. Danilov, B. Wittman, and S. Ganichev, *J. Electron. Mater.* **39**, 918 (2010).
- [29] S. V. Morozov, V. V. Rumyantsev, M. S. Zholudev, A. A. Dubinov, V. Y. Aleshkin, V. V. Utochkin, M. A. Fadeev, K. E. Kudryavtsev, N. N. Mikhailov, S. A. Dvoretzky, V. I. Gavrilenko, and F. Teppe, *ACS Photon.* **8**, 3526 (2021).
- [30] K. E. Kudryavtsev, V. V. Rumyantsev, V. V. Utochkin, A. A. Dubinov, V. Y. Aleshkin, M. S. Zholudev, N. N. Mikhailov, S. A. Dvoretzky, V. G. Remesnik, V. I. Gavrilenko, and S. V. Morozov, *J. Appl. Phys.* **133**, 074301 (2023).
- [31] M. Zholudev, F. Teppe, M. Orlita, C. Consejo, J. Torres, N. Dyakonova, M. Czapkiewicz, J. Wrobel, G. Grabecki, N. Mikhailov, S. Dvoretzky, A. Ikonnikov, K. Spirin, V. Aleshkin, V. Gavrilenko, and W. Knap, *Phys. Rev. B* **86**, 205420 (2012).
- [32] D. A. Dahl and L. J. Sham, *Phys. Rev. B* **16**, 651 (1977).
- [33] M. Grynberg, R. L. Toullec, and M. Balkanski, *Phys. Rev. B* **9**, 517 (1974).
- [34] D. N. Talwar and M. Vandevyver, *J. Appl. Phys.* **56**, 1601 (1984).
- [35] J. Baars and F. Sorger, *Solid State Commun.* **10**, 875 (1972).
- [36] V. Y. Aleshkin, A. A. Dubinov, and A. O. Rudakov, *Phys. Scr.* **98**, 065104 (2023).
- [37] D. N. Mirlin, in *Surface Polaritons: Electromagnetic Waves at Surfaces and Interfaces*, edited by V. M. Agranovich and D. L. Mills (North-Holland, Amsterdam, 1982).
- [38] L. D. Landau, J. Bell, M. Kearsley, L. Pitaevskii, E. Lifshitz, and J. Sykes, *Electrodynamics of Continuous Media* (Elsevier, Amsterdam, 2013), Vol. 8.
- [39] F. Giustino, *Rev. Mod. Phys.* **89**, 015003 (2017).
- [40] J. Pozhela, *Plasma and Current Instabilities in Semiconductors* (Pergamon Press, Oxford, 1981).
- [41] P. S. Kop'ev, D. N. Mirlin, D. G. Polyakov, I. I. Reshina, V. F. Sapega, and A. A. Sirenko, *Sov. Phys. Semicond.* **24**, 757 (1990).